scientific reports

Check for updates

OPEN

Structured transmittance illumination coherence holography

Aditya Chandra Mandal[1,2], Tushar Sarkar[1], Zeev Zalevsky[3] & Rakesh Kumar Singh[1]✉

The coherence holography offers an unconventional way to reconstruct the hologram where an incoherent light illumination is used for reconstruction purposes, and object encoded into the hologram is reconstructed as the distribution of the complex coherence function. Measurement of the coherence function usually requires an interferometric setup and array detectors. This paper presents an entirely new idea of reconstruction of the complex coherence function in the coherence holography without an interferometric setup. This is realized by structured pattern projections on the incoherent source structure and implementing measurement of the cross-covariance of the intensities by a single-pixel detector. This technique, named structured transmittance illumination coherence holography (STICH), helps to reconstruct the complex coherence from the intensity measurement in a single-pixel detector without an interferometric setup and also keeps advantages of the intensity correlations. A simple experimental setup is presented as a first step to realize the technique, and results based on the computer modeling of the experimental setup are presented to show validation of the idea.

Since its inception more than seventy years ago, holography offers a powerful tool for imaging and light synthesis[1–5]. Availability of high-quality array detectors and reconstruction algorithms has further revolutionized the holography, and optical reconstruction in the holography is replaced by the digital means, and technique is called digital holography (DH). The DH keeps inherent advantages of the holography concerning the complex amplitude distribution and additionally offers a simplified reconstruction of the hologram by a numerical means[5]. Conventional DH records and reconstructs the complex wavefield by an optical field distribution itself. The phase information of the wavefield is an important physical parameter of the light. Among various methods to recover the phase information, the DH is a well-established technique for quantitative phase imaging (QPI). Various QPI techniques have been developed, and significant among them are in-line, off-axis, and phase-shifting holography. In recent years, attempts have been made to improve the transverse spatial resolution in the DH by random[6–8] and structured light illumination[9–12]. Requirements to retrieve information from the self-luminous or incoherent object have also inspired new trends in the holography[13–19].

In a significant development, Takeda and co-workers have developed an unconventional holography called coherence holography (CH), where the information of the complex field is reconstructed as a distribution of the spatial coherence[20]. Here, the hologram is reconstructed by an incoherent light illumination rather than by a coherent light. The CH has opened new research directions on recording and shaping the spatial coherence for applications such as spatial coherence tomography, profilometry, imaging, and coherence current[21–25]. Principle of the CH is derived from the van Cittert-Zernike theorem, which connects the incoherent source structure with a far-field spatial coherence of the light. The main task in the CH is to design an appropriate interferometer for the measurement of spatial coherence. These interferometers mainly employ second-order correlation or fourth-order correlations measurement by the array detectors. In contrast to the interferometers based on the second-order correlations, the fourth-order correlation, i.e., intensity interferometers are highly stable for the coherence measurement[26]. Recently, Naik et al.[27] made use of the fourth-order correlation in the hologram, and technique is called a photon correlation holography (PCH). Basic principle of the PCH is derived from a connection between the cross-covariance of the intensities with the modulus square of the Fourier spectrum of the incoherent structure. However, phase information of the spectrum is lost in the PCH in contrast to the CH and DH techniques. Recovery of complex field parameters in the CH and DH is possible by employing an interferometer setup which makes the system bulky and prone to external disturbances and instabilities[2,22,24]. Recently, holographic methods based on interference of the coherence waves have been proposed to overcome the phase loss issue in the PCH experiments[28–33]. However, the interferometric systems bring bulkiness in the

[1]Laboratory of Information Photonics and Optical Metrology, Department of Physics, Indian Institute of Technology (Banaras Hindu University), Varanasi, Uttar Pradesh 221005, India. [2]Department of Mining Engineering, Indian Institute of Technology (Banaras Hindu University), Varanasi, Uttar Pradesh 221005, India. [3]Faculty of Engineering and Nano Technology Center, Bar-Ilan University, Ramat-Gan, Israel. ✉email: krakeshsingh.phy@iitbhu.ac.in

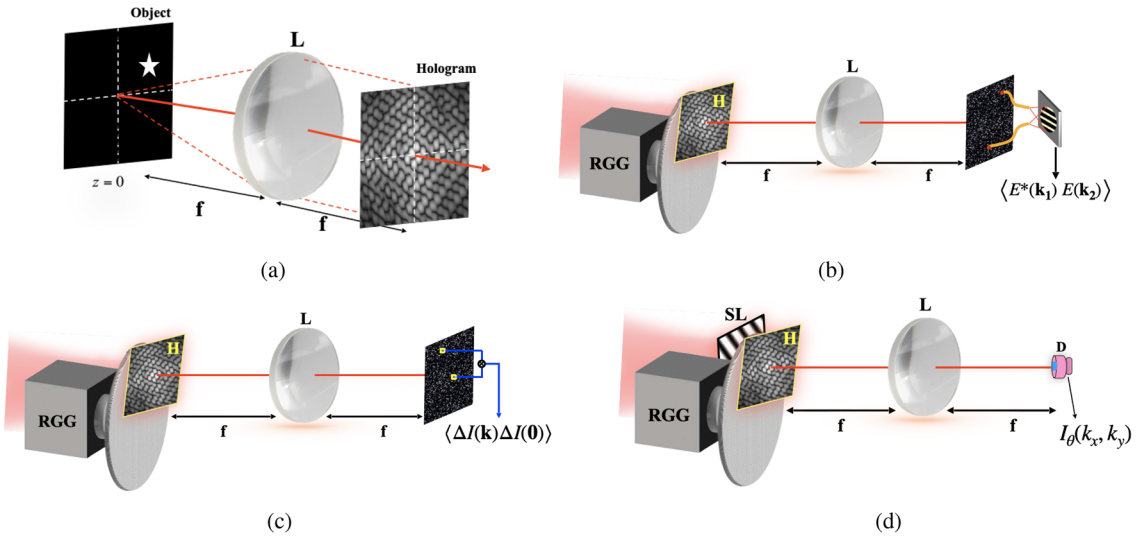

Figure 1. (**a**) Represents coherent recording of complex field of an object located at $Z = 0$, L is a lens with focal distance f (**b**) Represents the reconstruction process of the hologram with incoherent light, where L is a lens with focal distance f, RGG is rotating ground glass, H is hologram; (**c**) Represents the PCH setup: intensity correlation holography scheme; (**d**) Represents the STICH setup, where SL is structured light pattern, H is hologram, D is single-pixel detector.

experimental implementation and also require flexible control over the reference field to get the interference fringes in the cross-covariance function at the array detectors plane.

On the other hand, significant attempts have been made to develop computational imaging techniques such as single-pixel imaging with random and structured field illumination over the past few years[34–43]. In contrast to using conventional cameras and two-dimensional array detectors, single-pixel techniques make use of projection of light patterns onto a sample while a single-pixel detector measures the light intensity collected for each pattern. Therefore, stage of spatial sampling is moved from the camera to the programmable diffraction element where the structured patterns are loaded. Single-pixel imaging techniques have brought advantages such as use of a non-visible wavelength or precise time resolution, which can be costly and practically challenging to realize as a pixilated imaging device. Recently, a combination of optical and computation channels has been developed for the reconstruction of the three-dimensional (3D) amplitude object from a single-pixel detector, and technique is called hybrid correlation holography (HCH)[41]. This technique makes use of cross-covariance of the intensity and is derived from the connection between complex coherence function and intensity correlation for Gaussian random field. A new scheme based on the recovery of the complex-valued object in a modified HCH scheme with an interferometric setup has been developed[44].

In this paper, we present a new technique for the reconstruction of the complex field within the framework of the PCH and present a new theoretical basis for the reconstruction in correlation holography. This approach equips correlation imaging with a complete wavefront reconstruction without an interferometric setup but keeping the advantage of the intensity correlation. For this purpose, a structured light illumination is projected on the incoherent structure, and a far-field spectrum is measured by a single-pixel detector. A complex Fourier spectrum from the intensities is successfully obtained from the four-step phase shifting in the structured illumination. Although the Fourier spectrum measurement in the CH is based on the Hanbury Brown-Twiss (HBT) approach with a single-pixel detector but active illumination strategy in the proposed technique helps to overcome the phase loss problem of the typical HBT approach. Applying two-dimensional (2D) inverse Fourier transform (IFT) to the obtained spectrum yields the desired digital hologram. The phase-shifting illumination approach also brings the elimination of noise that is statistically the same. Moreover, such non-interferometric approach assisted with structured light illumination offers a new and stable method for imaging with incoherent light. A detailed theoretical foundation and implementation of the proposed technique in comparison to the CH and PCH are discussed below.

Basic principle

Basic principles of the CH and PCH have been discussed in detail in Ref.[20,27]. However, for the sake of continuity and to connect with basic principle of the proposed technique, we briefly describe the CH and PCH. Figure 1a represents a coherent recording of the complex field of an object in the Fourier hologram $H(r)$. The hologram $H(r)$ is a transparency that is read out with incoherent light, as shown in Fig. 1b for the CH. To describe the reconstruction process of the hologram in Fig. 1b, consider the complex field of light immediately behind the source as

$$E(r) = H(r)\exp[i\phi(r)] \tag{1}$$

where i denotes the imaginary unit and $H(r) = |H(r)|\exp[i\delta(r)]$ with $|H(r)|$ and $\delta(r)$ being the amplitude transmittance of the hologram and deterministic phase of the readout light, respectively. The spatial vector at the

source is $r \equiv (x, y)$. The random phase inserted in the light path to destroy spatial coherence by the rotating ground glass (RGG) is represented by $\phi(r)$ at a fixed time t. A lens in Fig. 1b with focal distance f is used to Fourier transform the randomly scatted light field from the source, and the complex field on the observation plane becomes

$$E(k) = \int E(r) \exp[-ik \cdot r] dr = \int H(r) \exp[i\phi(r)] \exp[-ik \cdot r] dr \tag{2}$$

where $k \equiv (k_x, k_y)$ is spatial frequency coordinate at the observation point. Two-point correlation of the random field is characterized as

$$\begin{aligned} W(k_1, k_2) &= \langle E^*(k_1) E(k_2) \rangle \\ &= \iint H^*(r_1) H(r_2) \langle \exp[i(\phi(r_2) - \phi(r_1))] \rangle \exp[-i(k_2 \cdot r_2 - k_1 \cdot r_1)] dr_2 dr_1 \end{aligned} \tag{3}$$

here $\langle . \rangle$ represents the ensemble average which will be replaced by the temporal average in the experiment. The rotating ground glass is considered to produce an incoherent source, i.e. $\langle \exp[i(\phi(r_2) - \phi(r_1))] \rangle \equiv \delta(r_2 - r_1)$. Considering $k_2 = k$ and $k_1 = 0$, Eq. (3) transforms into the van Cittert Zernike theorem as

$$F(k) = \int I(r) \exp[-ik \cdot r] dr \tag{4}$$

where $I(r) = |H(r)|^2$ is the source placed at the RGG plane and $F(k)$ represents the Fourier spectrum of the incoherent source at the far-field. It is important to mention that Eq. (4) connects an incoherent source structure at the RGG plane with the far-field complex coherence function and the source structure I(r) can be a hologram or any real source structure[30,45,46]. The complex spatial coherence function is used to record the incoherent object and develop a new kind of unconventional holography[20,45]. The basic principle of the CH is described by Eq. (4) and therefore provides reconstruction of the object as the distribution of the complex coherence function. The random field intensity at the observation plane, at a fixed time t corresponding to one rotation state of the RGG, is represented as

$$I(k) = |E(k)|^2 \tag{5}$$

The random intensity pattern $I(k)$ is having no direct resemblance to reconstruction of the object. The cross-covariance of the intensities of the Gaussian random field is given as[26]

$$\langle \Delta I(k) \Delta I(0) \rangle = |F(k)|^2 \tag{6}$$

where $\Delta I(k) = I(k) - \langle \Delta I(k) \rangle$ is the fluctuation of the intensities with respect to its average mean value. Eq. (6) highlights the basic principle of the PCH and is sketched in Fig. 1c, wherein the phase part of the coherence function is lost. To circumvent the issue of phase recovery with only measurement of the cross-covariance of the intensities, we here present a new technique called STICH. A basic principle of the STICH is represented in Fig. 1d and described as follows. A two dimensional (2-D) structured illumination with its spatial frequency (k_x, k_y) and initial phase θ is projected on the RGG. This structured illumination is a sinusoidal pattern and is represented as

$$P_\theta(x, y; k_x, k_y) = a + b \cdot \cos(k_x x + k_y y + \theta) \tag{7}$$

where a is an un-modulated term of the illumination pattern, and b represents the contrast. The light coming out of the structured transparency propagates through the RGG, which is used to mimic an incoherent light source. A hologram H is placed next to the RGG, as shown in Fig. 1d. Therefore, the instantaneous complex field immediately after the H is expressed as:

$$E_\theta(x, y; k_x, k_y) = H(x, y) \exp(i\phi(x, y)) \left(a + b \cdot \cos(k_x x + k_y y + \theta)\right) \tag{8}$$

The instantaneous complex field at the single-pixel detector is represented as

$$E_\theta(k_x, k_y) = E_n + w \iint_\Omega E_\theta(x, y; k_x, k_y) dx dy \tag{9}$$

where Ω represents the illuminated area, w is a scale factor whose value depends on the size and the location of the detector, E_n represents the response of background illumination. The instantaneous random intensity at the single-pixel detector is given as

$$I_\theta(k_x, k_y) = |E_\theta(k_x, k_y)|^2 \tag{10}$$

The random intensity variation from its mean intensity is calculated as

$$\Delta I_\theta(k_x, k_y) = I_\theta(k_x, k_y) - \langle I_\theta(k_x, k_y) \rangle \tag{11}$$

where the angular bracket $\langle . \rangle$ denotes the ensemble average and $\langle I_\theta(k_x, k_y) \rangle$ is mean intensity. The cross-covariance of the intensities is

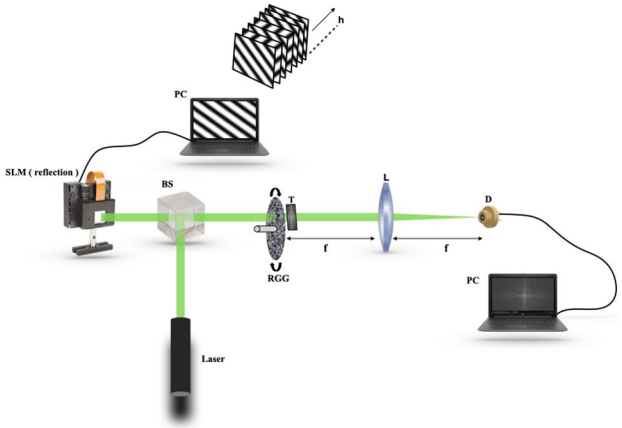

Figure 2. Experimental configuration: *BS* beam splitter, *SLM* spatial light modulator, *RGG* rotating ground glass, *T* transparency, *L* lens with focal distance *f*, *D* single-pixel detector, *PC* personal computer.

$$D_\theta\left(k_x,k_y\right)=\left\langle \Delta I_\theta\left(k_x,k_y\right)\Delta I_\theta\left(k_x,k_y\right)\right\rangle \tag{12}$$

The 4-step phase-shifting approach allows extraction of the complex Fourier coefficient $F(k_x,k_y)$ by combination of four cross-covariance fuctions of the intensities D_0, $D_{\pi/2}$, D_π , $D_{3\pi/2}$ corresponding to the illumination patterns, and the fourier coefficient $F(k_x,k_y)$ is represented as[34]

$$\begin{aligned}&\left[D_0\left(k_x,k_y\right)-D_\pi\left(k_x,k_y\right)\right]+i\cdot\left[D_{\pi/2}\left(k_x,k_y\right)-D_{3\pi/2}\left(k_x,k_y\right)\right]\\&=2bw\iint_\Omega I(x,y)\cdot\exp\left[-i\left(k_xx+k_yy\right)\right]dxdy\end{aligned} \tag{13}$$

The Fourier coefficient is expressed as

$$\begin{aligned}&F\left(k_x,k_y\right)=\iint_\Omega I(x,y)\cdot\exp\left[-i\left(k_xx+k_yy\right)\right]dxdy\\&=\frac{1}{2bw}\left[D_0\left(k_x,k_y\right)-D_\pi\left(k_x,k_y\right)\right]+i\cdot\left[D_{\pi/2}\left(k_x,k_y\right)-D_{3\pi/2}\left(k_x,k_y\right)\right]\end{aligned} \tag{14}$$

By computing Fourier coefficients F (i.e., the Fourier spectrum) using Eq. (14) for a complete set of (k_x,k_y), the desired complex field distribution is reconstructed. A 4-step phase-shifting sinusoid illumination plays an essential role in the proposed technique and helps to reconstruct the incoherently illuminated hologram in the CH. Eq. (13) can not only assemble the Fourier spectrum of the desired incoherent source structure but also eliminate undesired direct current (DC) terms.

Experimental design and algorithm

A possible experimental design for the proposed technique is shown in Fig. 2. A monochromatic collimated laser light is folded by a beam splitter (BS) and incident on a spatial light modulator (SLM). The SLM in Fig. 2 is considered to be a reflective type and loaded with the h number of sinusoidal patterns in a sequence.

The sinusoidal pattern displayed to the SLM is inserted into the incident beam, and subsequently, this structured light transmits through the BS and illuminates the RGG. The RGG introduces randomness in the incident structured light. As shown in Fig. 1a, a computer-generated hologram of an off-axis object is used as transparency and placed adjacent to the RGG. The structured pattern embedded in the stochastic field due to the RGG illuminates a hologram $H(x, y)$. Scattering of the light through the RGG generates a stochastic field with the Gaussian statistics. The scattered light further propagates and is Fourier transformed by a lens L at the single-pixel detector plane D. Corresponding to the spatial frequency and initial phase of the loaded structured pattern, an instantaneous random field at the single-pixel detector is represented by $E_\theta\left(k_x,k_y\right)$. The instantaneous signal at the detector is represented as $|E_\theta\left(k_x,k_y\right)|^2$. After the single-pixel measurement for a particular random phase mask, we stored the value in our personal computer (PC) for post-processing. Due to the Gaussian statistics, the cross-covariance of the intensities is estimated at the single-pixel corresponding to different sets of random phase masks introduced by the RGG. The cross-covariance of the intensities at the single-pixel detector for a given frequency pair (k_x,k_y) and initial phase θ is represented as $D_\theta\left(k_x,k_y\right)$. For a complete set of Fourier coefficients, we illuminate the hologram $H(x, y)$ by the structured patterns with full sets of spatial frequency (k_x,k_y). Each complex Fourier coefficient corresponding to that spatial frequency is extracted by using a 4-step phase-shifting approach. The number of Fourier coefficients in the Fourier domain is the same as the number of pixels in the spatial domain.

The algorithm proposed in this paper is an iterative heuristic that aims to reconstruct complex object encoded into the hologram as the distribution of the complex coherence function. In contrast to the previously reported CH, here we report the use of the structured illumination at the RGG plane. This strategy makes reconstruction procedure completely different from previously developed reconstruction methods and also equips us to extract the complex field even from a single-pixel detector. This is a unique feature of our proposed technique

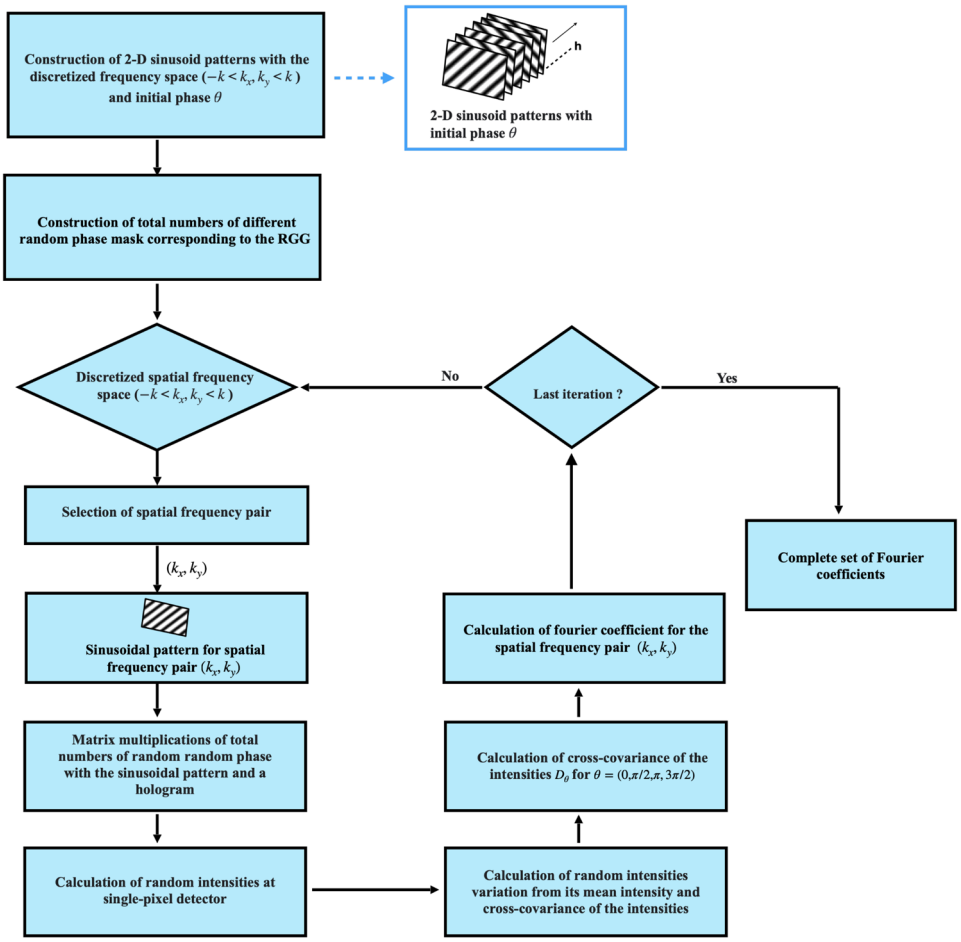

Figure 3. Proposed STICH algorithm steps.

that helps to recover the complex coherence without interferometry. The algorithm in our work is implemented using MATLAB and simulated on a personal computer. Figure 3 shows the steps of the algorithm, which are:

1. A hologram of size $N \times N$ pixels is taken as transparency.
2. Construction of sinusoidal patterns and random phase masks :
   (a) Total M number of different random phase masks of same size of hologram are generated.
   (b) The 2-D sinusoidal patterns of size $N \times N$ pixels with initial phase $\theta = (0, \pi/2, \pi, 3\pi/2)$ are constructed by considering discretized spatial frequency space $-k < k_x, k_y < k$.
3. Iterative steps:
   (a) First, a 2-D sinusoidal pattern for that particular frequency pair (k_x, k_y) is taken. A single-pixel detector is used to sense the random light field (matrix multiplication of hologram and sinusoidal pattern and random phase mask), and corresponding random intensity is represented using Eq. (10).
   (b) In such a way, other intensity patterns at single-pixel detector corresponding to different sets of random phase masks introduced by the RGG are obtained. Random intensity variations from its mean intensity are calculated using Eq. (11). Cross-covariance of the intensity for the taken spatial frequency pair (k_x, k_y) is calculated using Eq. (12).
   (c) Calculation of each complex valued Fourier coefficient $F(k_x, k_y)$ corresponding to the spatial frequency pair is simulated from four cross-covariance fuctions of the intensities $D_\theta(\theta = 0, \pi/2, \pi, 3\pi/2)$ (see Eq. 14).

For the complete set of desired $R \times R$ size Fourier coefficients, we need to iterate the above steps over the discretized spatial frequency space unless the last iteration is obtained. Total $4R^2 (= 4 \times R \times R)$ number of sinusoidal patterns need to be projected, including the four-step phase-shifting by an SLM shown in Fig. 2, on which the patterns are controlled by a personal computer (PC) directly. A Fourier coefficients $F(k_x, k_y)$

	M = 200	M = 500	M = 1000
(I)	$v = 4.86$	$v = 5.36$	$v = 11.10$
	$\eta = 0.69$	$\eta = 0.71$	$\eta = 0.84$
(II)	$v = 5.11$	$v = 6.15$	$v = 18.39$
	$\eta = 0.70$	$\eta = 0.74$	$\eta = 0.90$

Table 1. Visibility (v) and reconstruction efficiency (η) .

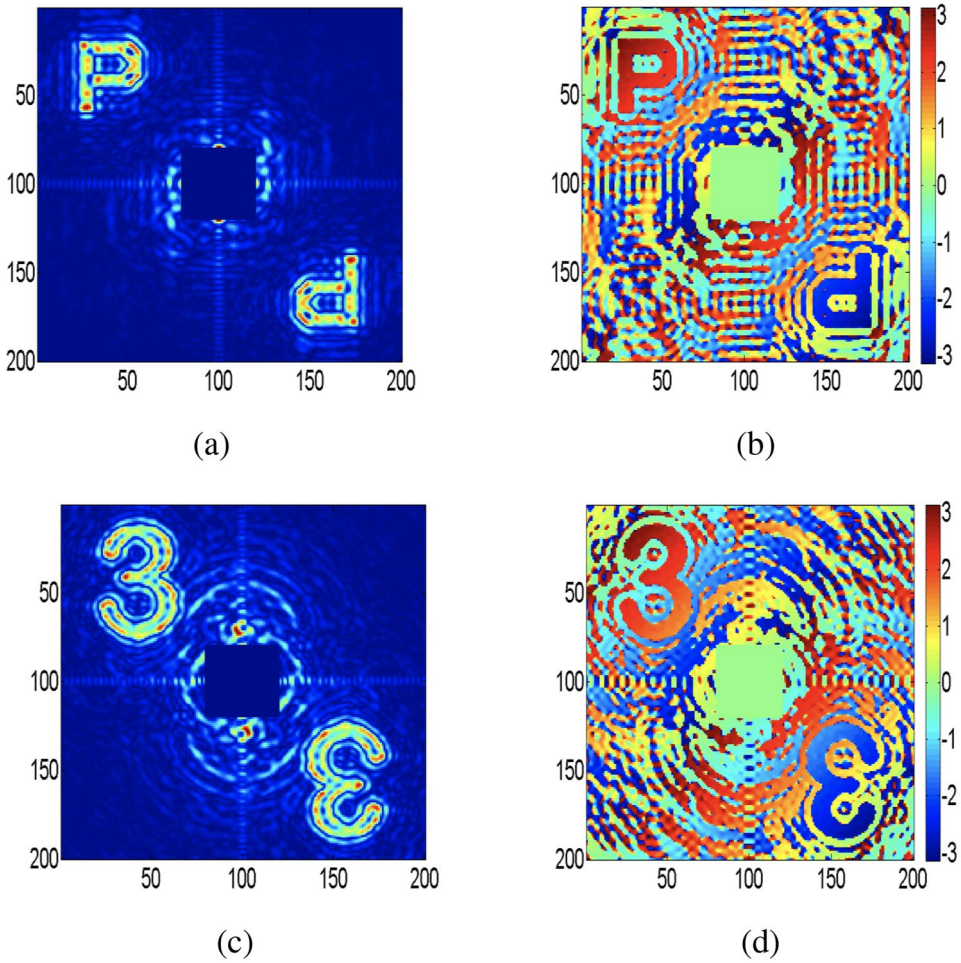

Figure 4. Recovery of complex fields without RGG from holograms of objects, letter "P" and number "3" (**a**) Amplitude distribution of letter "P" (**b**) Phase distribution of letter "P" (**c**) Amplitude distribution of number "3" (**d**) Phase distribution of number "3".

is obtained with 4 measurements. So, basically, for fully sampling $R \times R$ size Fourier coefficients consumes $4 \cdot R^2 \cdot M (= 4 \times R \times R \times M)$ measurements of single-pixel detector to reconstruct the complex object.

Results

Here, we present computational results processed using MATLAB for the validation of our proposed experimental design. The phase information of the wavefield is a critical parameter to examine a complex field of an object. Figure 4a–d show both amplitude and phase distributions of objects, letter "P" and number "3" respectively, which are directly reconstructed from DH. Applying two-dimensional Fourier transform on the DH brings out three spectra: a non-modulating central DC term, the desired off-axis spectrum, and its conjugate. Location of an off-axis spectrum is governed by carrier frequency as shown in recording of DH in Fig. 1a. The unwanted DC term containing high-frequency content is digitally suppressed in Fig. 4 to highlight the objects located in an off-axis position. Figures 5 and 6 represent the reconstructed complex fields from holograms using the STICH technique at different numbers of random phase masks (M) and the quality of reconstruction depends on the

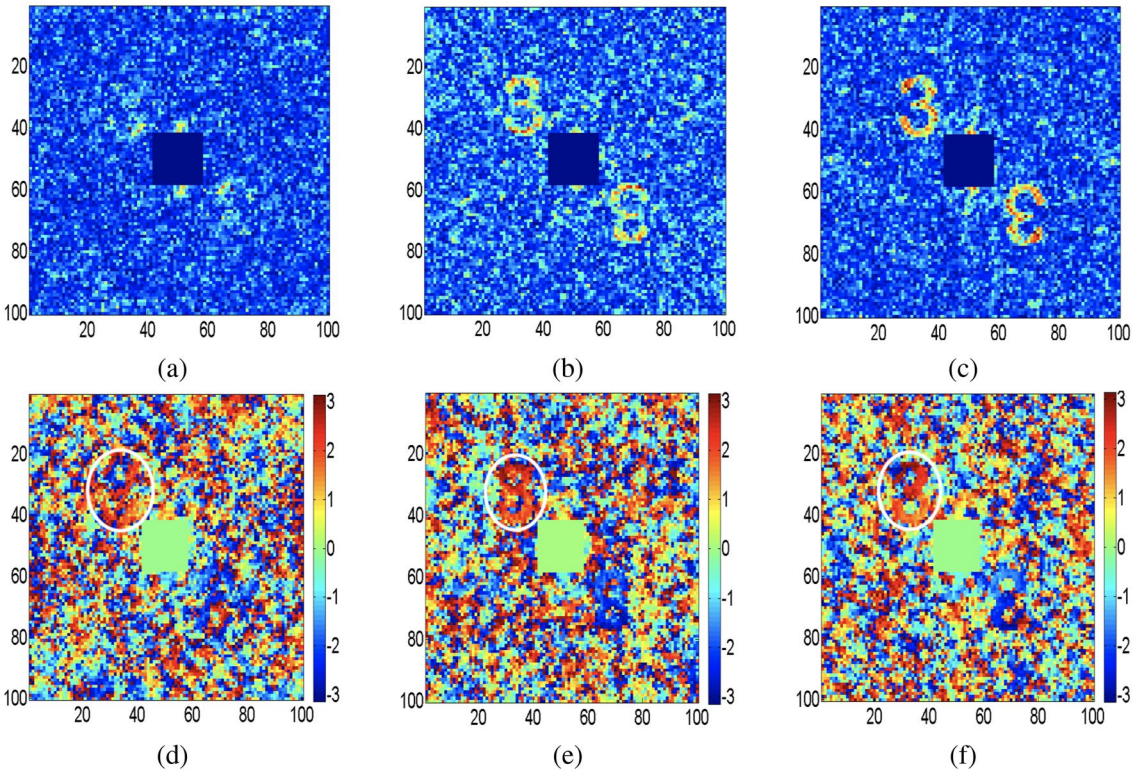

Figure 5. Recovery of the complex fields using STICH for three different M values: an off-axis hologram of number "3" is used as transparency (**a**, **d**) Amplitude and phase distribution of object for $M = 200$; (**b**,**e**) Amplitude and phase distribution of object for $M = 500$; (**c**,**f**) Amplitude and phase distribution of object for $M = 1000$.

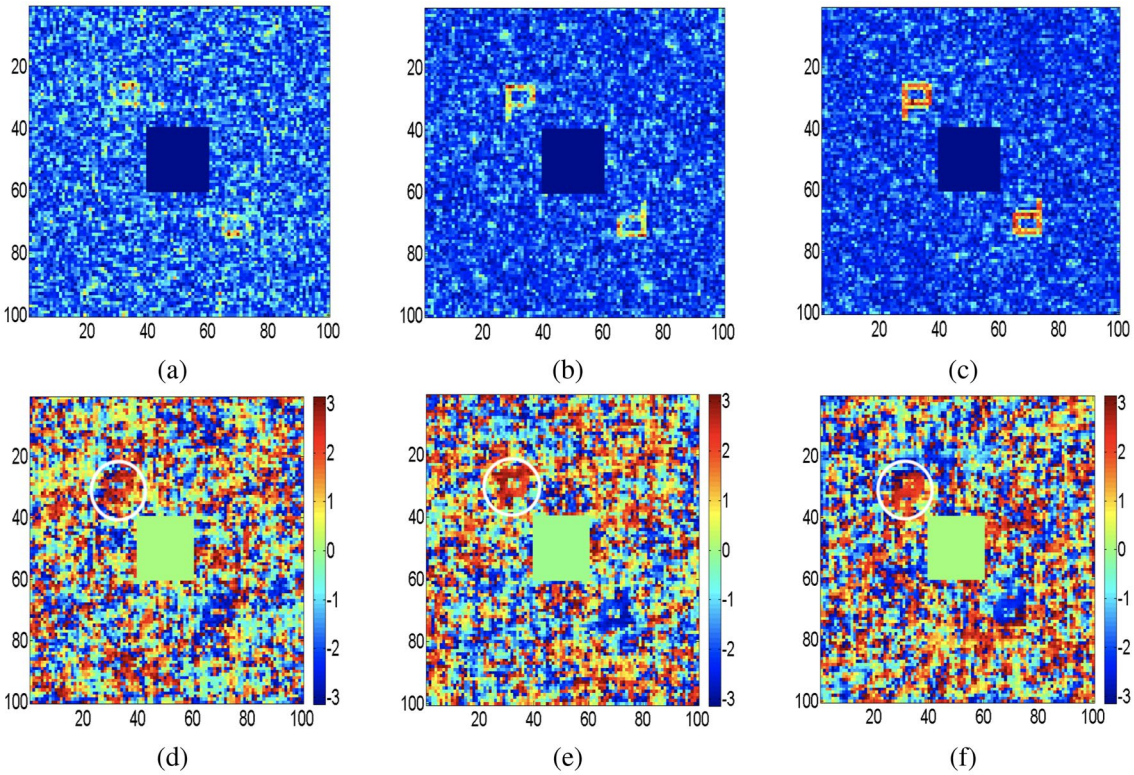

Figure 6. Recovery of the complex fields using STICH for three different M values: an off-axis hologram of letter "P" is used as transparency (**a**,**d**) Amplitude and phase distribution of object for $M = 200$; (**b**,**e**) Amplitude and phase distribution of object for $M = 500$; (**c**,**f**) Amplitude and phase distribution of object for $M = 1000$.

value of M. In order to examine the effect of M on reconstruction quality of STICH, we evaluate visibility (ν) and reconstruction efficiency (η)[47] for three different numbers of $M = (200, 500, 1000)$ and results are given in Table 1. Amplitude and phase distributions of number "3" are shown in Fig. 5a–f for $M = (200, 500, 1000)$. Similarly for letter "P", Fig. 6a–f show the amplitude and phase distributions for $M = (200, 500, 1000)$. In both object's reconstruction central DC terms are digitally suppressed as shown in Figs. 5 and 6. The central DC in the reconstruction appears because of use of an off-axis hologram as the transparency. The visibility of a target reconstruction is defined as the degree to which it can be distinguished from background noise. It is calculated as the ratio of the average image intensity level in the signal region to the average background intensity level. Here Otsu's method[48] is used as a global threshold to identify the signal region.

In order to reconstruct complex fields of size 100×100 from hologram of size 200×200 using STICH, structured illumination patterns are generated according to Eq. (7), where $a = 0.5, b = 0.5$, spatial frequencies range is $-2.5 \leq (k_x, k_y) \leq 2.5$ at steps of 0.0505.

The calculated visibility value for Fig. 4a,c are 127.6 and 64.7. The calculated visibility and reconstruction efficiency value for Fig. 5a–c and for Fig. 6a–c are given in Table 1. (I) and (II) respectively. The upper part of conjugate phase distributions in Figs. 5 and 6 are highlighted with white color ring. From Table 1 and Figs. 5 and 6, it can be seen that reconstruction quality improves with increase of value of M. Number of sinusoidal patterns required to be projected for the reconstruction of complex coherence function can be reduced using the compressed sensing approach[49]. Moreover, automated coupling of the SLM with the single-pixel detector is expected to simplify the experimental implementation of the proposed work.

Conclusion

In conclusion, a new technique entitled STICH is presented to reconstruct the complex coherence from the intensity measurement with a single-pixel detector and without an interferometric setup. This brings the advantages of compatibility in the reconstruction of complex fields in the correlation-based imaging system. An experimental configuration and computational model of it are described to validate our idea. We have demonstrated the reconstructions of complex fields of objects at different random phase masks and the quality of reconstruction depends on the value of number of random phase masks used to realize the thermal light source. Furthermore, the proposed technique is capable to image the incoherent source at the scattering plane from the reconstructed complex coherence function. This incoherent source may appear as a hologram or non-hologram prior to the random scattering. Therefore, basic principle of structured light illumination for the coherence holography is expected to provide new direction on the holography with incoherent light and imaging through scattering medium.

Received: 22 September 2021; Accepted: 20 January 2022
Published online: 16 March 2022

References

1. Gabor, D. A new microscopic principle. *Nature* **161**, 777–778 (1948).
2. Leith, E. N. & Upatnieks, J. Reconstructed wavefronts and communication theory. *JOSA* **52**, 1123–1130 (1962).
3. Yamaguchi, I. Phase-shifting digital holography. In *Digital Holography and Three-Dimensional Display* 145–171 (Springer, 2006).
4. Poon, T. .-C. . & Liu, J. .-P. *Introduction to Modern Digital Holography: with MATLAB* (Cambridge University Press, 2014).
5. Schnars, U. & Jüptner, W. *Digital Holography: Digital Hologram Recording, Numerical Reconstruction, and Related Techniques* (Springer, 2005).
6. Park, Y. *et al.* Speckle-field digital holographic microscopy. *Opt. Express* **17**, 12285–12292 (2009).
7. Vinu, R., Chen, Z., Pu, J., Otani, Y. & Singh, R. K. Speckle-field digital polarization holographic microscopy. *Opt. Lett.* **44**, 5711–5714 (2019).
8. Choi, Y. *et al.* Dynamic speckle illumination wide-field reflection phase microscopy. *Opt. Lett.* **39**, 6062–6065 (2014).
9. Gao, P., Pedrini, G. & Osten, W. Structured illumination for resolution enhancement and autofocusing in digital holographic microscopy. *Opt. Lett.* **38**, 1328–1330 (2013).
10. Ma, J., Yuan, C., Situ, G., Pedrini, G. & Osten, W. Resolution enhancement in digital holographic microscopy with structured illumination. *Chin. Opt. Lett.* **11**, 090901 (2013).
11. Micó, V., Zheng, J., Garcia, J., Zalevsky, Z. & Gao, P. Resolution enhancement in quantitative phase microscopy. *Adv. Opt. Photon.* **11**, 135–214 (2019).
12. Gao, P. *et al.* Recent advances in structured illumination microscopy. *J. Phys. Photon.* **2**, 2 (2021).
13. Rosen, J. & Brooker, G. Digital spatially incoherent fresnel holography. *Opt. Lett.* **32**, 912–914 (2007).
14. Tahara, T., Kanno, T., Arai, Y. & Ozawa, T. Single-shot phase-shifting incoherent digital holography. *J. Opt.* **19**, 065705 (2017).
15. Bouchal, P., Kapitán, J., Chmelík, R. & Bouchal, Z. Point spread function and two-point resolution in fresnel incoherent correlation holography. *Opt. Express* **19**, 15603–15620 (2011).
16. Rosen, J. & Brooker, G. Fluorescence incoherent color holography. *Opt. Express* **15**, 2244–2250 (2007).
17. Quan, X., Matoba, O. & Awatsuji, Y. Single-shot incoherent digital holography using a dual-focusing lens with diffraction gratings. *Opt. Lett.* **42**, 383–386 (2017).
18. Watanabe, K. & Nomura, T. Recording spatially incoherent fourier hologram using dual channel rotational shearing interferometer. *Appl. Opt.* **54**, A18–A22 (2015).
19. Rosen, J., Brooker, G., Indebetouw, G. & Shaked, N. T. A review of incoherent digital fresnel holography. *J. Hologr. speckle* **5**, 124–140 (2009).
20. Takeda, M., Wang, W., Duan, Z. & Miyamoto, Y. Coherence holography. *Opt. Express* **13**, 9629–9635 (2005).
21. Duan, Z., Miyamoto, Y. & Takeda, M. Dispersion-free optical coherence depth sensing with a spatial frequency comb generated by an angular spectrum modulator. *Opt. Express* **14**, 12109–12121 (2006).
22. Takeda, M., Wang, W., Naik, D. N. & Singh, R. K. Spatial statistical optics and spatial correlation holography: a review. *Opt. Rev.* **21**, 849–861 (2014).
23. Naik, D. N., Ezawa, T., Singh, R. K., Miyamoto, Y. & Takeda, M. Coherence holography by achromatic 3-d field correlation of generic thermal light with an imaging sagnac shearing interferometer. *Opt. Express* **20**, 19658–19669 (2012).
24. Soni, N. K., Vinu, R. & Singh, R. K. Polarization modulation for imaging behind the scattering medium. *Opt. Lett.* **41**, 906–909 (2016).

25. Wang, W. & Takeda, M. Coherence current, coherence vortex, and the conservation law of coherence. *Phys. Rev. Lett.* **96**, 223904 (2006).
26. Goodman, J. W. *Statistical Optics* (John Wiley & Sons, 2015).
27. Naik, D. N., Singh, R. K., Ezawa, T., Miyamoto, Y. & Takeda, M. Photon correlation holography. *Opt. Express* **19**, 1408–1421 (2011).
28. Singh, R. K., Sharma, M.A.,. Recovery of complex valued objects from two-point intensity correlation measurement. *Appl. Phys. Lett.* **104**, 111108 (2014).
29. Singh, R. K., Vyas, S. & Miyamoto, Y. Lensless fourier transform holography for coherence waves. *J. Opt.* **19**, 115705 (2017).
30. Kim, K. *et al.* Imaging through scattering media using digital holography. *Opt. Commun.* **439**, 218–223 (2019).
31. Somkuwar, A. S., Das, B., Vinu, R., Park, Y. & Singh, R. K. Holographic imaging through a scattering layer using speckle interferometry. *JOSA A* **34**, 1392–1399 (2017).
32. Chen, L., Singh, R. K., Chen, Z. & Pu, J. Phase shifting digital holography with the hanbury brown-twiss approach. *Opt. Lett.* **45**, 212–215 (2020).
33. Chen, L., Chen, Z., Singh, R. K., Vinu, R. & Pu, J. Increasing field of view and signal to noise ratio in the quantitative phase imaging with phase shifting holography based on the hanbury brown-twiss approach. *Opt. Lasers Eng.* **148**, 106771 (2022).
34. Zhang, Z., Ma, X. & Zhong, J. Single-pixel imaging by means of fourier spectrum acquisition. *Nat. Commun.* **6**, 1–6 (2015).
35. Martínez-León, L. *et al.* Single-pixel digital holography with phase-encoded illumination. *Opt. Express* **25**, 4975–4984 (2017).
36. Horisaki, R., Matsui, H., Egami, R. & Tanida, J. Single-pixel compressive diffractive imaging. *Appl. Opt.* **56**, 1353–1357 (2017).
37. Edgar, M. P., Gibson, G. M. & Padgett, M. J. Principles and prospects for single-pixel imaging. *Nat. Photonics* **13**, 13–20 (2019).
38. Shin, S., Lee, K., Baek, Y. & Park, Y. Reference-free single-point holographic imaging and realization of an optical bidirectional transducer. *Phys. Rev. Appl.* **9**, 044042 (2018).
39. Hu, X. *et al.* Single-pixel phase imaging by fourier spectrum sampling. *Appl. Phys. Lett.* **114**, 051102 (2019).
40. Ota, K. & Hayasaki, Y. Complex-amplitude single-pixel imaging. *Opt. Lett.* **43**, 3682–3685 (2018).
41. Singh, R. K. Hybrid correlation holography with a single pixel detector. *Opt. Lett.* **42**, 2515–2518 (2017).
42. Gibson, G. M., Johnson, S. D. & Padgett, M. J. Single-pixel imaging 12 years on: a review. *Opt. Express* **28**, 28190–28208 (2020).
43. Sarkar, T. *et al.* Correlation holography with a single-pixel detector: A review. *Laser Optoelectron. Progr.* **58**, 1011011 (2021).
44. Chen, Z., Singh, D., Singh, R. K. & Pu, J. Complex field measurement in a single pixel hybrid correlation holography. *J. Phys. Commun.* **4**, 045009 (2020).
45. Naik, D. N., Pedrini, G. & Osten, W. Recording of incoherent-object hologram as complex spatial coherence function using sagnac radial shearing interferometer and a pockels cell. *Opt. Express* **21**, 3990–3995 (2013).
46. Singh, R. K., Vinu, R. P. V. K. & Sharma, M. S. A. Retrieving complex coherence from two-point intensity correlation using holographic principle. *Opt. Eng.* **53**, 104102 (2014).
47. Hillman, T. R. *et al.* Digital optical phase conjugation for delivering two-dimensional images through turbid media. *Sci. Rep.* **3**, 1–5 (2013).
48. Otsu, N. A threshold selection method from gray-level histograms. *IEEE Trans. Syst. Man Cybern.* **9**, 62–66 (1979).
49. Saluja, R., Subrahmanyam, G., Mishra, D., Vinu, R. & Singh, R. K. Compressive correlation holography. *Appl. Opt.* **56**, 6949–6955 (2017).

Acknowledgements

The work is supported by the Science and Engineering Research Board (SERB) India- CORE/2019/000026 and Department of Biotechnology (DBT)- BT/PR35557/MED/32/707/2019. T.S acknowledges support from University Grant Commission (UGC), India for his scholarship.

Author contributions

A.C.M. conceived of idea and build the theoretical basis, experimental design, and completed simulation and preparation of manuscript. T.S. involved in experimental design, simulation, preparation of manuscript. Z.Z. provided advice and assistance, reviewing and editing the work. R.K.S. was involved in supervision, formulation of research goals and aims, funding acquisition, reviewing, and editing.

Competing interests

The authors declare no competing interests.

Additional information

Correspondence and requests for materials should be addressed to R.K.S.